

Alkylation of Gold Surface by Treatment with $C_{18}H_{37}HgOTs$ and Anodic Hg Stripping

Malgorzata Mucha,[†] Eva Kaletová,[†] Anna Kohutová,[†] Frank Scholz,[‡] Elizabeth S. Stensrud,[†] Ivan Stibor,[†] Lubomír Pospíšil,^{†,§} Florian von Wrochem,[‡] and Josef Michl^{†,||,*}

[†]Institute of Organic Chemistry and Biochemistry, Academy of Sciences of the Czech Republic, Flemingovo nám. 2, 16610 Prague 6, Czech Republic

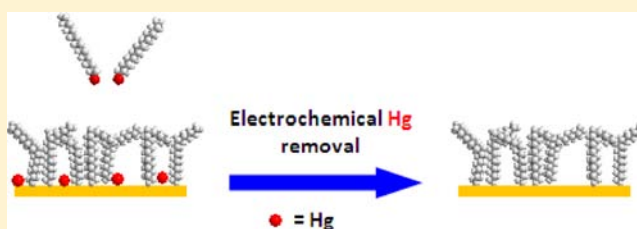
[‡]Sony Deutschland GmbH, Materials Science Laboratory, Hedelfinger Strasse 61, 70327 Stuttgart, Germany

[§]J. Heyrovský Institute of Physical Chemistry, Academy of Sciences of the Czech Republic, Dolejškova 3, 18223 Prague, Czech Republic

^{||}Department of Chemistry and Biochemistry, University of Colorado, 215 UCB, Boulder, Colorado 80309-0215, United States

Supporting Information

ABSTRACT: Treatment of a gold surface with a solution of $C_{18}H_{37}HgOTs$ under ambient conditions results in the formation of a covalently adsorbed monolayer containing alkyl chains attached directly to gold, Hg(0) atoms, and no tosyl groups. It is stable against a variety of chemical agents. When the initial deposition is performed at a positive applied potential and is followed by oxidative electrochemical stripping, the mercury can be completely removed, leaving a gold surface covered only with alkyl chains. The details of the attachment structure are not known. The conclusions are based on infrared spectroscopy, X-ray and UV photoelectron spectroscopy, ellipsometry, contact angle goniometry, differential pulse polarography, and measurements of electrode blocking and electrochemical admittance.



INTRODUCTION

It has been recently reported^{1,2} that disordered monolayers form on gold surface upon treatment with solutions of trialkylstannyl tosylates, trifluoroacetates, or triflates under ambient conditions. This discovery was preceded and motivated by accidental observations of attachment of organomercury salts to the surface of gold^{3–5} and even earlier investigations of adsorption of organoplatinum complexes to platinum.⁶ The results indicated that such behavior may have some generality and that other organometallics should be examined, but trialkylsilyl derivatives were found to be unreactive. At the time, it was established that the leaving group did not remain in the monolayer, but no direct information on the mode of attachment of the adsorbate to the gold surface was available. We have since found that the process can be extended to additional structural types of organometallics, carrying various main group metals.⁷ The organic groups are detached from the metal atom during their transfer to the gold surface, and under ambient conditions the metal usually ends up as an oxide. Complementary evidence for transfer of alkyl groups from alkyltrimethylstannanes to the atoms of a gold surface resulted from recent independent measurements of single-molecule conductivity,^{8,9} and dovetails with our findings.

Presently, we take a closer look at the behavior of an organomercurial, $C_{18}H_{37}HgOTs$, and report spectroscopic and

electrochemical evidence that a treatment of a gold surface with a solution of *n*-octadecylmercuric tosylate under ambient conditions covers the surface with a monolayer that consists of *n*-octadecyl groups and mercury in its elemental form, and contains no tosylate. The adsorbed atomic mercury can be removed by oxidative anodic stripping, leaving a coating of alkyl groups on an otherwise clean gold surface. Elsewhere,¹⁰ we report analogous monolayer formation with C_4H_9HgOTs and find that the removal of elemental mercury from the initially formed surface monolayers can be accomplished by thermal annealing of the monolayer. At this time, we do not have direct spectroscopic evidence for the detailed structure of the direct attachment of the alkyl groups to the surface. The simplest possibility is a single alkyl-Au bond, but we cannot exclude a loss of one or more hydrogen atoms from the terminal or penultimate carbons of the alkyl chain and more complex bonding patterns such as alkylidene-Au₂, etc.

The use of main group organometallics for the direct transfer of organic residues to gold surface promises to complement the established application of thiols^{11–17} and analogous compounds^{18–20} that produces monolayers in which carbon is believed to be attached to the gold surface through a mediating atom such as sulfur. Each choice appears to have certain

Received: December 5, 2012

Published: February 11, 2013

disadvantages (for thiols, sensitivity to aerial oxidation has been noted^{21–23}), and a wider selection of options is likely to be useful.

RESULTS

Monolayer Formation and Ellipsometric Characterization. Figure 1 compares the gradual increase of the

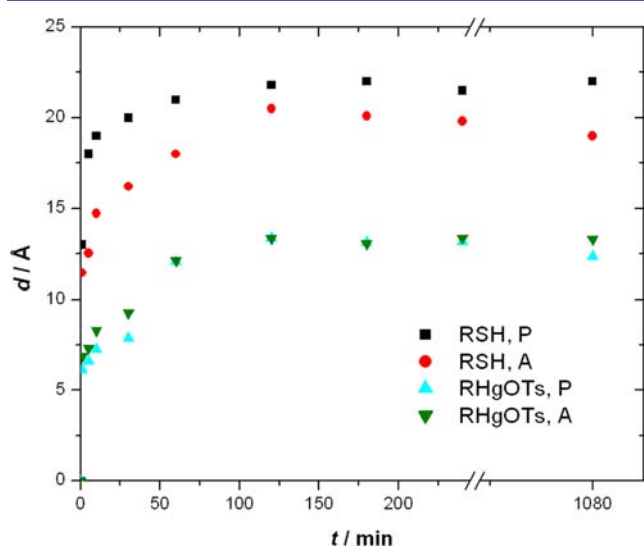


Figure 1. Kinetics of monolayer formation followed by ellipsometric thickness d for $C_{18}H_{37}HgOTs$ (blue \blacktriangle , green \blacktriangledown) and $C_{18}H_{37}SH$ (black \blacksquare , red \bullet) on gold substrates cleaned by piranha (P) and hydrogen flame annealing (A).

ellipsometric thickness of the surface layers formed from 10^{-5} M solutions of $C_{18}H_{37}HgOTs$ in THF and $C_{18}H_{37}SH$ in ethanol. In both instances, the adsorption process is self-limiting, and the growth of the adsorbed layer stops after about two hours at an ellipsometric thickness of ~ 13 Å for $C_{18}H_{37}HgOTs$ and ~ 21 Å for $C_{18}H_{37}SH$, regardless of whether the gold surface was first cleaned with a hydrogen flame or a piranha solution. Although the growth limit is reached after about 2 h in both cases, the ellipsometrically determined initial rate of growth of the monolayer is faster with $C_{18}H_{37}SH$ than with $C_{18}H_{37}HgOTs$. At 10^{-3} M $C_{18}H_{37}HgOTs$ concentration the same limiting thickness is reached in ~ 1.5 h.

Contact Angle Goniometry. Contact angles of water on monolayers from $C_{18}H_{37}HgOTs$ are $96^\circ \pm 4^\circ$ and $101^\circ \pm 2^\circ$ when the gold substrates are cleaned by hydrogen flame or piranha solution, respectively. They are distinctly higher than the $17 \pm 3^\circ$ and $71 \pm 4^\circ$ angles measured on the initial gold substrate cleaned by hydrogen flame or piranha, respectively, and are similar to the values 92 – 97° found for layers generated from trialkylstannyl precursors.¹ The angle is significantly lower than the 113° we observe for a monolayer from $C_{18}H_{37}SH$ adsorbed on gold cleaned by piranha and close to the 100° we observe for a $C_{18}H_{37}SH$ monolayer on flame-annealed gold.

Infrared Spectroscopy (IR). Single-reflection attenuated total reflectance (ATR) IR spectra contain the typical peaks of alkyl chains (Figure 2A) and those of the tosylate residue are absent.

The spectra show only vibrations attributable to the CH_3 and CH_2 groups: stretching at 2853 , $\nu_s(CH_2)$, 2871 , $\nu_s(CH_3)$, 2925 , $\nu_{as}(CH_2)$, and 2958 , $\nu_{as}(CH_3)$, and bending at 1378 , 1418 , and 1468 (all in cm^{-1}). As in the monolayers from trialkylstannyl

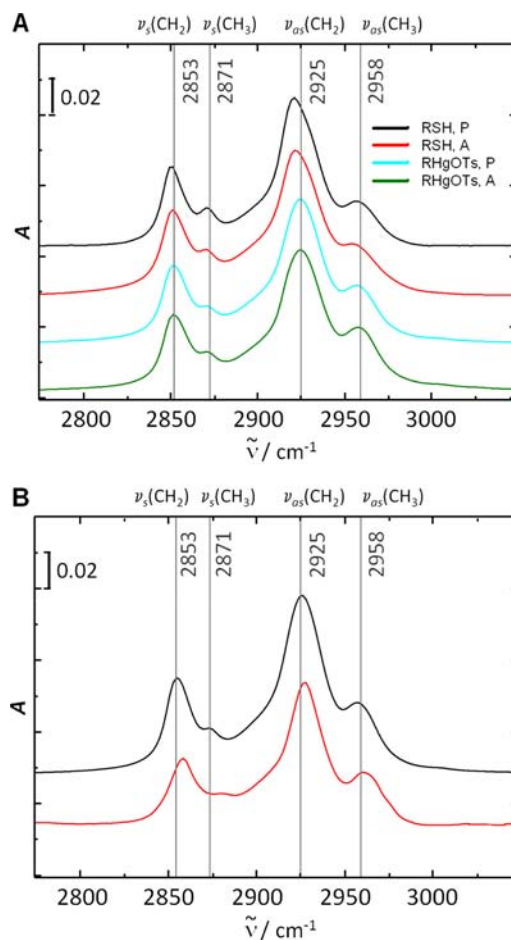


Figure 2. ATR-FTIR spectra. (A) $C_{18}H_{37}SH$ (black and red) and $C_{18}H_{37}HgOTs$ (cyan and green) based monolayers adsorbed on gold substrates cleaned by piranha (P) and hydrogen flame annealing (A). (B) Au plate treated with $C_{18}H_{37}HgOTs$ before (black) and after (red) electrochemical stripping.

compounds,¹ $\nu_s(CH_2)$ occurs 5 cm^{-1} and $\nu_{as}(CH_2)$ 6 cm^{-1} above their respective locations in the highly ordered monolayer of 1-octadecanethiol, suggesting that the alkyl chain are not all-anti, but disordered. Upon heating, the monolayer formed from octadecanethiol becomes disordered and the symmetric and antisymmetric CH_2 stretches move to higher frequencies. In the octadecylmercury derived monolayer, these bands are already shifted at room temperature and no further shift occurs upon heating. As expected, the peaks due to CH_2 vibrations dominate considerably over those due to CH_3 vibrations, more so than they do for monolayers obtained from C_4H_9HgOTs (Supporting Information, SI).

Photoelectron Spectroscopy: X-ray (XPS) and UV (UPS). X-ray photoelectron spectra show the presence of Hg and C and the absence of S at the gold surface in a fully grown $C_{18}H_{37}HgOTs$ derived monolayer, hence the tosylate residue is lost from $C_{18}H_{37}HgOTs$ during the self-assembly process, similarly as it is from organostannyl tosylates.¹ An O 1s peak is usually also present and its intensity varies considerably from sample to sample. In the XP spectra of the pristine monolayers, the Hg atoms yield only a single set of peaks both in the $4f$ and in the $4d$ regions. The core level energies (99.67 eV for Hg $4f_{7/2}$) fit the expectations for elemental Hg.^{24,25}

The stability of the Hg signals in time as a function of temperature was investigated separately on very similar samples

Table 1. XPS Results for Monolayers from C₁₈H₃₇HgOTs

| sample | R (Hg/Au) ^a | R (C/Au) ^a | A (Hg)/A ^{2b} | A (C ₁₈)/A ^{2b} | E _{Hg 4f7/2} /eV ^c | E _{Hg 4d5/2} /eV ^c | E _{C 1s} /eV ^c |
|-----------------------|------------------------|-----------------------|------------------------|--------------------------------------|--|--|------------------------------------|
| initial | 0.073 | 0.64 | 13 | 36 | 99.67 | 358.16 | 284.63 |
| stripped ^d | | 0.68 | | 34 | | | 284.50 |

^aElemental ratios from XPS peak areas after correction for instrumental sensitivity factors and for attenuation from the Hg and S layers (attenuation factor is 0.69 for a dense Hg layer as in the initial SAM). ^bArea/atom and area/molecule obtained by comparison of Hg/Au and C/Au ratios with S/Au ratios of densely packed alkanethiol monolayers³⁶ (S/Au \approx 0.045, area/molecule = 21.6 Å²) and by consideration of the photoemission attenuation due to the organic layer, respectively. ^cChemical shifts derived from peak centers of Gaussian/Lorentzian fits to the XPS data. ^dAu on mica cleaned with butane flame was kept 3 h at a potential of +1 V in 10⁻⁵ M C₁₈H₃₇HgOTs in 0.1 M tetra-*n*-butylammonium hexafluorophosphate in THF in the dark at room temperature under Ar, bathed in THF, immersed in aqueous 0.1 M KF and kept at +1 V for 1 h, rinsed, bathed in water, and dried under a stream of nitrogen.

produced by treatment of a gold surface with C₄H₉HgOTs.¹⁰ In high vacuum, the signals are stable indefinitely at ambient temperature and up to \sim 60 °C, but begin to disappear rapidly at \sim 90 °C, and are inobservable above 120 °C. The disappearance of Hg from the surface is presumably due to diffusion into the bulk, but evaporation may contribute as well. The stability of the Hg signals at room temperature is important for the present purposes because it permits us to use their intensities for a quantitation of the relative amounts of Hg and C present. The results are collected in Table 1 and sample spectra are shown in Figure 3.

The Hg 4*d* signals appear at binding energies of 358.16 eV (shoulder) and 378.06 eV for the 5/2 and the 3/2 components,

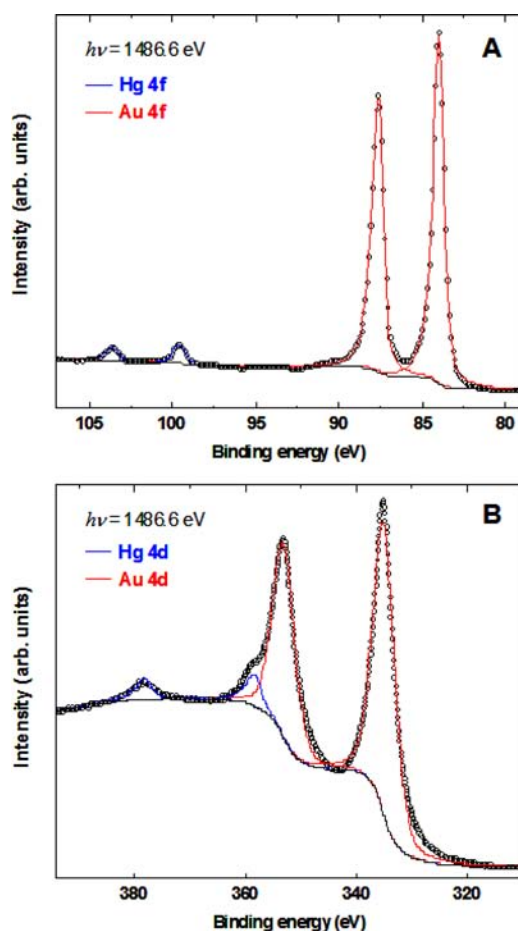


Figure 3. XPS in the Hg 4*f* (panel A) and Hg 4*d* (panel B) regions for monolayers formed by the treatment of gold surface with C₁₈H₃₇HgOTs. Symbols represent data points, lines (red and blue) are fitted curves. The black line is the background.

respectively. The Hg 4*d* peaks are partially overlapped by strong Au 4*d* signals from the gold substrate at 334.98 and 353.09 eV (Au 4*d*_{5/2} and Au 4*d*_{3/2}, respectively). A fit to the data, subject to peak area constraints imposed by angular momentum rules, permits an evaluation of Hg abundance at the surface, assuming equal attenuation of Au and Hg photoelectrons by the alkyl chain overlayer. With these assumptions, consistent results are obtained for Hg 4*d* and Hg 4*f* lines. A comparison of the XPS intensity ratios of Hg and Au signals in C₁₈H₃₇Hg SAMs with the intensity ratios of S and Au signals in densely packed dodecanethiol monolayers, which we use as a reference, yields an area of \sim 13 Å² per Hg atom for C₁₈H₃₇Hg SAMs. This corresponds to an Hg surface density that is roughly twice as high as that of sulfur atoms in alkanethiol monolayers. The C 1*s* and Hg 4*f* signal intensities indicate however that the surface concentration of carbon is about 3 times lower than what is expected based on Hg density and on molecular composition (C₁₈H₃₇Hg). Overall, the surface density of C₁₈ units on Au is about 40% lower than in densely packed alkanethiols.

The location of the C 1*s* peak at a binding energy of 284.5 eV is in good agreement with its position in alkanes. In some samples a weak peak appeared at 288 eV, presumably due to a carbonyl carbon. The relative abundance of surface-bound carbon (or carbons) is too low for them to be discerned as a peak with a chemical shift different from the others.

The UV photoelectron spectrum (SI, Figure S9) of the monolayer produced with C₁₈H₃₇HgOTs (no Hg stripping) is very similar to that of a monolayer produced with dodecanethiol and shows the characteristic alkyl valence band structure.

Chemical Stability. Chemical stability of the C₁₈H₃₇HgOTs derived monolayers was examined by monitoring the loss of their IR absorbance between 2800 and 3000 cm⁻¹ as a function of time after exposure either to the laboratory atmosphere for a week or to various solvents and reagents overnight. It is similar to the stability of monolayers produced from trialkylstannyl precursors¹ and generally slightly lower than that of monolayers obtained with C₁₈H₃₇SH (Figure 4). Only the resistance to oxidants is significantly higher. Even after the monolayers are partially or fully desorbed, no new absorption bands appear. There is not much difference between the two gold cleaning procedures. In a sense, a stability comparison to monolayers obtained with C₁₈H₃₇SH is unfair since the latter are denser and less permeable (cf. electrode blocking below). It is conceivable that at similar density monolayers composed of directly bound alkyls would be considerably more resistant than thiolate monolayers. This is not an issue that we can address presently and present Figure 4 primarily as evidence that the alkyl groups in our monolayers

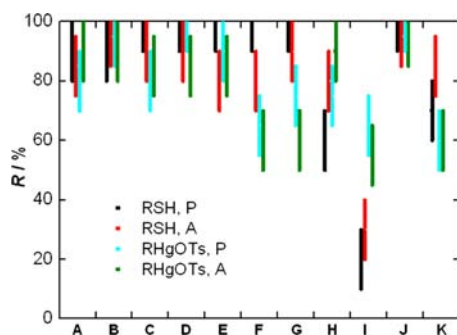


Figure 4. Stability of adsorbed monolayers from $C_{18}H_{37}SH$ (black and red bars) and from $C_{18}H_{37}HgOTs$ (cyan and green bars) on gold surface after 20–23 h immersion at room temperature, followed by rinsing and drying. R is the percent monolayer remaining on the gold surface, calculated as the ratio of the final to the initial integrated intensity of the 2800–3000 cm^{-1} bands. (A) Dry CH_2Cl_2 , (B) wet CH_2Cl_2 , (C) n -hexane, (D) ethanol, (E) water, (F) 0.1 M H_2SO_4 , (G) 0.1 M $NaOH$, (H) 1 mM $KMnO_4$, (I) 30% H_2O_2 , (J) 10 mM $NaBH_4$, and (K) 7 days in laboratory air. Gold substrates cleaned by piranha (P) and hydrogen flame annealing (A).

are attached strongly and not by mere physisorption. Some of the CH stretch intensity may be due to relatively easily removed adventitious impurities and the chemisorbed monolayer may be sturdier than Figure 4 suggests.

Electrochemistry. The electrochemical stability range is similar for monolayers derived from $C_{18}H_{37}HgOTs$ (−1.38 to +1.40 V) and $C_{18}H_{37}SH$ (−1.33 to +1.40 V). Cyclic voltammetry with aqueous $[Fe(CN)_6]^{3-}/[Fe(CN)_6]^{4-}$ as a redox probe shows that the layer deposited from $C_{18}H_{37}HgOTs$, like those obtained from trialkylstannyl compounds,¹ reduces the cyclic voltammetric peak height to about two-thirds with respect to a cleaned Au sample (the electrode surface is ~35% blocked, Figure 5A). Since the electron transfer rate constant of $[Fe(CN)_6]^{3-}/[Fe(CN)_6]^{4-}$ is high, cyclic voltammetry may not be sensitive enough to the change of the electron transfer rate due to the blocking. A more sensitive method is impedance spectroscopy, which yields the charge transfer resistance of fast electron transfer reactions, derived from the radius of a semicircle of the electrode impedance plot. The impedance method can detect rate changes that are still within the diffusion controlled limit on the time scale of voltammetry. Indeed, already a qualitative inspection indicates a substantial increase of the semicircle relative to the one obtained on a cleaned Au surface (Figure 5B).

The blocking is incomplete even after an overnight immersion in a solution of $C_{18}H_{37}HgOTs$, whereas a 2-h immersion in a solution of $C_{18}H_{37}SH$ is sufficient to produce a monolayer that completely suppresses the electrochemical response (Figure 5A).

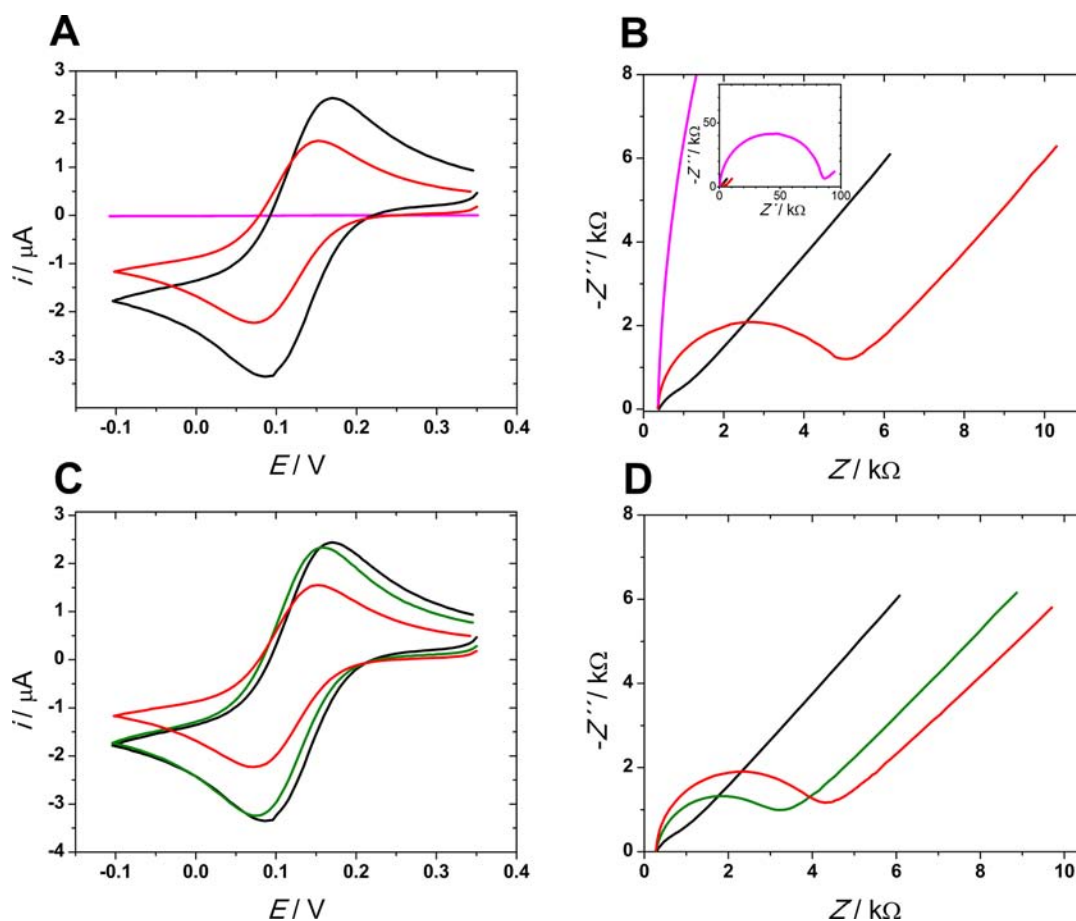


Figure 5. Aqueous solution of 2 mM $K_3[Fe(CN)_6]$ and 0.1 M KNO_3 . (A) Cyclic voltammetry and (B) local complex impedance plot of a 4.02 mm^2 spot on a Au plate (virgin, black; with an adsorbed layer of $C_{18}H_{37}HgOTs$, red; and with an adsorbed layer of $C_{18}H_{37}SH$, magenta). (C) Cyclic voltammetry and (D) local complex impedance plot of an Au plate (virgin, black; with an adsorbed layer of $C_{18}H_{37}HgOTs$, red; and after electrochemical Hg stripping, green).

A more detailed electrochemical examination of the adsorbed monolayer took advantage of the known properties of the Hg(0)/Hg(II) redox couple on gold electrode (Figure S1 in the SI). In aqueous media, its potential lies at about 0.1 V against the Ag|AgCl|3 M LiCl electrode.²⁷ It was considered important to perform the electrochemical measurements on the very same flat plates covered with a thin layer of Au that were used for other measurements, such as IR and XPS. A special electrochemical cell that permits a measurement on a selected 4.02 mm² area of the plate was designed for the purpose (SI, Figures S2 and S3). We verified that results obtained in this fashion were similar to those obtained on Au disc electrodes embedded in a glass capillary. The measured complex electrochemical impedance is shown in the SI (Figure S4).

Successive scans by differential pulse polarography (DPP)²⁸ yielded mercury oxidation signals of gradually decreasing size (Figure S5 of the SI), suggesting that elemental mercury was being removed. A determination averaged over four different spots on a plate yielded a peak potential value of $+135 \pm 5$ mV and peak current of 11.9 ± 4.4 nA at an area of 4.02 mm².

When potential steps from -0.1 to $+0.3$ V were applied to an Au surface covered with a monolayer produced with C₁₈HgOTs and immersed into an aqueous 0.1 M KNO₃ solution (immersed area 0.32 cm²), transient currents i decayed in time (t) as $1/t$ (SI Figure S6), demonstrating that the current transient is not controlled by diffusion from the bulk of the solution and that the decay corresponds to the oxidation of surface confined Hg atoms. A similar hyperbolic i - t dependence for an adsorbed species has been described before.²⁹ Numerical integration yielded a charge of 48 mC, which contains faradaic (Q_F) and double layer (Q_C) contributions. Repetition of the experiment with a cleaned Au surface of the same area yielded $Q_C = 12.9$ mC. The charging current decayed exponentially in time (SI Figure S6). From $Q_F = 35.1$ mC, the surface concentration of Hg atoms is 1.14×10^{-9} mol/cm², or 1 Hg atom per 15 Å².

Electrochemical Stripping of Mercury. A suitable stripping potential of 0.3 V against the Ag|AgCl|3 M LiCl electrode was estimated from the DPP results. When it was applied to the whole electrode for 1 h, the DPP peak of mercury disappeared, but XPS indicated that 65% of the elemental Hg remained on the surface. Repeated scans of E from -1.0 V to $+1.4$ V lead to a gradual decrease of the double layer capacitance C between -1 V and $+1$ V to a very low value, suggestive of 100% coverage by a fairly compact layer (Figure 6). The decrease is especially apparent at positive potentials, whereas at negative potentials the initial capacitance is already smaller. The capacitance values show that outside this range C₁₈H₃₇HgOTs is still adsorbed to some extent, in a form of a less compact adsorbate.

The C - E plots contain a sharp AC peak at 0.5 V against the Ag|AgCl|3 M LiCl electrode, absent at early and late times. Complex impedance at the potential of the peak maximum as a function of the applied frequency (SI Figure S4) is a semicircle connected to a mass transfer line, implying that the removal of mercury is a kinetically controlled process (for numerical fitting, see SI). A cyclic voltammogram and a complex impedance plot of an Hg-stripped sample are shown in Figure S3C,D.

The results obtained on gold electrodes are quite unlike those obtained on a glassy carbon electrode, which we expect to be inert (SI Figure S7). On carbon, the admittance data show no maximum and no substantial time evolution of the

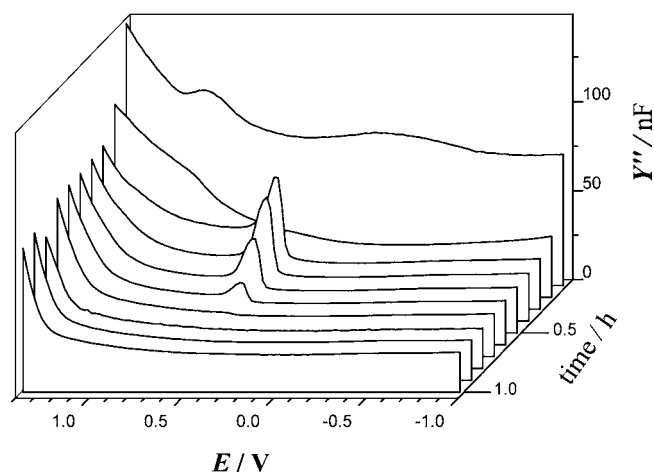


Figure 6. Imaginary component of Au electrode admittance in 0.2 mM C₁₈H₃₇HgOTs in acetonitrile and 0.1 M *n*-Bu₄PF₆. AC frequency: 64 Hz; amplitude: 5 mV. Voltage scan start: -1.0 V.

adsorption zones upon repeated voltage scans. Admittance at positive potentials never reaches very low and potential-independent values.

The results shown in Figure 6 suggested an improved protocol for possible electrochemical removal of Hg from the surface. In a series of experiments, Au plates were immersed for 2 h in a C₁₈H₃₇HgOTs solution. The plate was then transferred to an electrochemical cell filled with 0.1 M TBAPF₆ and a potential of 1.0 V was applied for 1 h. XPS analysis indicated that the content of Hg on the surface dropped to about 20% of the original value.

An even higher degree of Hg removal was achieved by initially immersing the Au plate in the electrochemical cell containing 10^{-5} M C₁₈H₃₇HgOTs and in 0.1 M TBAPF₆ in THF and allowing the monolayer formation to take place at 1.0 V for a period of 4 h. The plate was then rinsed with THF and kept at a potential of 1.0 V in a 0.1 M solution of TBAPF₆ in acetonitrile or in a 0.1 M solution of KF in water for approximately 1 h. This procedure yielded an adsorbed layer containing no detectable Hg (at most 5% of the original content) but still containing the C 1s peak, demonstrating the presence of the monolayer (Figure 7, Table 1).

Properties of Hg-Free Monolayers. The electrochemical removal of Hg on gold originally cleaned by a hydrogen flame decreased the ellipsometric thickness of monolayer from ~ 13 to 9 Å and reduced the contact angle to $\sim 53^\circ$. The C 1s XPS data (Figure 7) confirmed that the same amount of carbon was still present after electrochemical stripping.

IR spectra taken after the electrochemical Hg stripping resemble those taken before the stripping. Stretching vibrations are observed at 2853, $\nu_s(\text{CH}_2)$; 2871, $\nu_s(\text{CH}_3)$; 2925, $\nu_{\text{as}}(\text{CH}_2)$; and 2958, $\nu_{\text{as}}(\text{CH}_3)$; all in cm⁻¹, with $\nu_s(\text{CH}_2)$ and $\nu_{\text{as}}(\text{CH}_2)$ 3 cm⁻¹ above their respective locations before the stripping (Figure 2B). Bending vibrations are seen at 1378, 1418, and 1468 cm⁻¹.

DISCUSSION

Pristine Monolayers. The formation of a monolayer on a gold surface upon treatment with a solution of C₁₈H₃₇HgOTs under ambient conditions proceeds well but more slowly than the formation of a monolayer from C₁₈H₃₇SH (Figure 1). The ellipsometric thickness is smaller, only about ~ 13 instead of

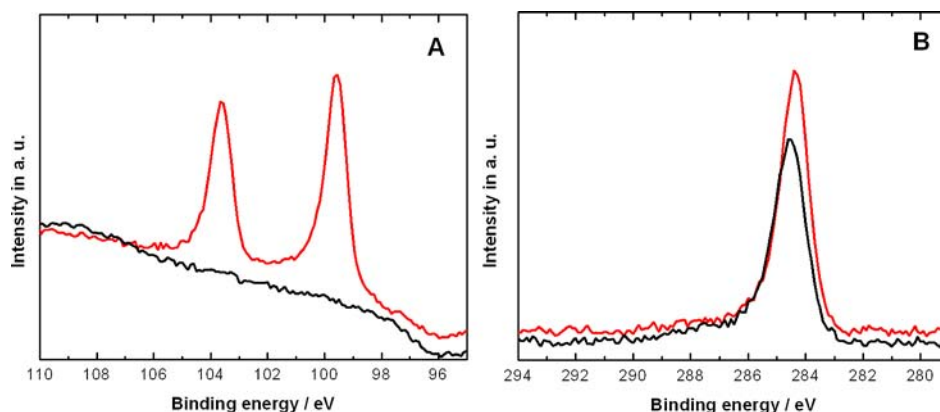


Figure 7. XPS in the Hg 4f (panel A) and C 1s (panel B) regions of a Au substrate treated with $C_{18}H_{37}HgOTs$ before (red) and after (black) electrochemical stripping of Hg.

~ 21 Å, and the monolayers are slightly less resistant to most chemical reagents tested and more resistant to oxidants. The ~ 13 Å thickness of the alkylmercury-based monolayer derived from ellipsometry is probably fairly reliable since the refractive index of the monolayer is not likely to be affected much by the presence of Hg on the gold surface (but might be affected by a reduced packing density of the chains).

The ~ 13 Å thickness contrasts with the ellipsometric thickness of the various trialkylstannyl-derived monolayers, which was only 6–7 Å,¹ and suggests a considerably denser coverage for alkylmercury-derived monolayers. However, this thickness is clearly smaller than that of alkanethiol-based monolayers. This would be expected if the alkyl chains are attached directly to the surface gold atoms and if some of the surface area is blocked by Hg atoms, reducing the coverage by alkyl chains. From contact angle goniometry, the alkylmercury-derived monolayer surface is found to be hydrophobic, consistent with methyl termination.

From both IR and XPS data, the tosylate leaving group is absent and alkyl chains are present. Their presence is also apparent in UPS and IR. The observed IR frequencies are not compatible with an all-anti alkyl conformation and suggest the presence of disordered chains. Disorder is also suggested by the poor electrode blocking properties of the monolayer.

From both XPS and DPP data, the surface contains a large amount of elemental mercury before the electrochemical stripping. The position of the narrow XPS peaks in the spectrum exactly matches the binding energy of elemental mercury^{24,25} and gives no indication, within the 0.1 eV resolution for peak centers, that Hg is present in more than one kind of environment. The polarographic peak corresponds to Hg(0)/Hg(II) oxidation. The areas per mercury atom deduced from the two methods are similar, ~ 13 (XPS) and 15 (DPP) Å²/Hg atom. The $Q_F = 35.1$ mC value probably underestimates the amount of Hg present, since some of the surface area is blocked by the adsorbed layer, and the electrochemical value of 15 Å²/Hg atom is an upper limit, whereas the XPS value of 13 Å²/Hg atom is more reliable. To derive the latter value, equal attenuation of Hg 4f and Au 4f photoelectrons by the alkyl overlayer is assumed and the attenuation from the Hg layer is explicitly included. An Hg adlayer on Au has precedent from a previous study of underpotential deposition.³⁰

The surface area per alkyl chain deduced from the C 1s XPS signal is ~ 36 Å²/chain. This is about 66% more than the area

per sulfur atom and thus per alkyl chain in a close-packed dodecanethiolate monolayer, which is 21.6 Å²/S atom,³¹ and roughly 3 times the surface area per Hg atom. Since small differences in molecular coverage can strongly affect the chain tilt angle, the reduced thickness observed by ellipsometry is easily explained by the lower packing density, under the assumption that the $C_{18}H_{37}$ chains are attached directly to Au.

The factor of ~ 3 observed between the surface areas of ~ 13 Å²/Hg atom and 36 Å²/alkyl chain precludes the possibility that each single mercury atom carries an alkyl chain. Although about 1/3 of the Hg atoms could be attached to an alkyl chain based on the evidence discussed so far, it would be unlikely for XPS signals from Hg atoms in $C_{18}H_{37}Hg$ to be identical with the signals from elemental Hg within the 0.1 eV resolution. It appears most probable that during the self-assembly some of the alkyl chains shift from Hg to Au whereas the remaining alkyls are desorbed. We have no spectroscopic evidence for the mode of attachment of the alkyl group to the surface gold atoms, and the simplest such attachment would be through a single C–Au bond. An analogous alkyl shift from an Sn atom to a Au surface, inducing C–Au bond formation, has been proposed recently to explain observations of enhanced single-molecule conductivity in alkyl chains.^{8,9}

The compactness of an adsorbed monolayer is usually tested by its inhibiting properties. Simple electron transfer reactions, such as the one-electron exchange in $[Fe(CN)_6]^{3-/4-}$, often show a complete elimination of the faradaic current. This is not true in the present case and the monolayer produced by deposition of $C_{18}H_{37}HgOTs$ only blocks $\sim 35\%$ of the surface. The anodic and cathodic peak potentials are practically unchanged. This observation is in agreement with standard assumptions concerning the influence of uncharged surfactants on the electron transfer rate.^{32,33}

According to a simplified model, the effective electron transfer rate constant k_{eff} is a linear function of the degree of coverage θ ,

$$k_{eff} = k_0(1 - \theta) + k_1\theta$$

where k_0 is the rate constant on the free surface and k_1 is the rate constant on a fully covered surface. Our observation suggests that prior to the electrochemical stripping treatment on the Hg-covered parts of the Au surface k_0 is as high as on bare Au and the voltammetric peak separation is unchanged. Alkyl chains block the electron transfer and reduce the active electrode area, causing a decrease of voltammetric peak heights

(Figure 5). The rate constant k_1 is very likely small, since otherwise a larger separation of voltammetric peaks would be detected. The removal of Hg from the adsorbed layer will not have much effect on the total active area but may lead to a more evenly distributed adsorbate and to a higher porosity of the surface layer. The voltammograms show an almost negligible inhibition, but simulations show that for all heterogeneous rate constants higher than $0.01 \text{ cm} \cdot \text{s}^{-1}$ identical voltammograms are obtained. The application of a faster technique, impedance spectroscopy, revealed that the electron transfer is inhibited even after the removal of Hg from the adsorbed layer (Figure S5C,D).

Similarly as the detailed nature of the attachment of the alkyl chains to the surface gold atoms, the mechanism by which they are transferred from the Hg atom to the Au atom or atoms is not known. There seems to be little if any precedent for the process. A distant analogy might be drawn to gas-phase S_N2 reactions in which a nucleophile such as NH_3 displaces a metal atom M ($M = \text{Zn}, \text{Cd}, \text{or Hg}$) from a carbon in the ion CH_3M^+ to yield CH_3NH_3^+ .³⁴ In our case, the Au surface would act as a nucleophile and the displacement would occur on the α carbon of $\text{C}_{18}\text{H}_{37}\text{HgOTs}$, which would act as $\text{C}_{18}\text{H}_{37}\text{Hg}^+ \text{TsO}^-$ to yield $\text{Au}_n^+ - \text{C}_{18}\text{H}_{37} + \text{Hg} + \text{TsO}^-$. Instances in which a gold atom³⁵ or a small gold cluster^{36,37} located on a surface acts as an electron donor are known.

Monolayers after Oxidative Mercury Stripping. The imaginary component of electrode admittance is proportional to the double layer capacitance C and sensitively responds to the structure of the interface. Comparison of repeated scans from -1.0 V to $+1.4 \text{ V}$ measured without and with $\text{C}_{18}\text{H}_{37}\text{HgOTs}$ in the bulk of the solution shows a remarkable gradual decrease of the double layer capacitance C in the presence of the adsorbate (Figure 6) as the layer adsorbed to the surface becomes progressively more compact, until at the end the capacitance is very low and almost potential independent. This is characteristic of a compact layer.^{38,39} The slow initial growth of the peak at 0.5 V in Figure 7 is attributed to a relatively slow formation of the initial monolayer.

The attribution of the admittance maximum at 0.5 V to electrochemical stripping of Hg is supported by the shape of the complex impedance plot (SI Figure S4), which implies a kinetically controlled process, most likely electron transfer from Hg hindered by the adsorbed layer and shifted to a higher potential relative to DPP on a clean surface. The disappearance of the maximum at the end of the stripping experiment suggests that the removal of Hg ceases.

IR and XPS show that after stripping, alkyl chains are still adsorbed to the surface, although the mercury is desorbed. At this point, most or all alkyls must be directly connected to the gold surface atoms, even those previously attached to the Au surface through Hg atoms, if there were any. The ellipsometric thickness is reduced upon stripping, and this is assigned to the loss of an important constituent of the original monolayer, elemental Hg. From the present data, it is however not at all obvious that the alkyls are attached to the surface through a single C–Au bond.

CONCLUSIONS

In conclusion, we have demonstrated that the treatment of a gold surface with a solution of $\text{C}_{18}\text{H}_{37}\text{HgOTs}$ produces sturdy monolayers containing elemental mercury and disordered alkyl chains, attached directly to gold surface atoms in an unknown

mode. Oxidative stripping removes the mercury from the monolayer, and when it is started concurrently with the deposition, it leaves no detectable mercury on the surface. The result is a layer of n -octadecyl chains attached to an otherwise clean gold surface.

EXPERIMENTAL SECTION

WARNING. Organomercury compounds are highly toxic and require the use of protective garments and extreme care in handling. Contact with skin must be carefully avoided. Waste needs to be treated separately from ordinary laboratory waste and disposed of properly.

Materials. Octadecylmercury(II) Bromide (1). Magnesium (100 mg, 4 mmol) was heated to $340 \text{ }^\circ\text{C}$ under reduced pressure for several minutes. After cooling to room temperature by flow of argon, a small piece of iodine was added. The flask was heated again until it turned purple ($250 \text{ }^\circ\text{C}$). Octadecyl bromide (1.0 g, 3 mmol) and tetrahydrofuran (5 mL) were added. The solution was refluxed for 2 h, cooled, filtered through glass wool, and slowly added to a solution of HgBr_2 (1.1 g, 3 mmol) in dry diethyl ether. After being stirred overnight at room temperature under argon atmosphere, chloroform (50 mL) was added and the solution was filtered over diatomaceous earth. The solid was washed with chloroform and combined filtrates were evaporated to give crude product (1.6 g), which was then recrystallized twice from hexanes. Yield 0.9 g (56%). Mp $112.0\text{--}114.0 \text{ }^\circ\text{C}$ (lit.⁴⁰ $110\text{--}111 \text{ }^\circ\text{C}$). Elemental analysis: calcd.: 40.49% C, 6.98% H; found: 40.16% C, 6.82% H. $^1\text{H NMR}$ (CDCl_3) δ 0.88 (t, $J = 7 \text{ Hz}$, CH_3 , 3H), 1.21–1.39 (m, s CH_2 , 28H), 1.57 (br s, CH_2 , 2H), 1.78 (quintet, $J = 7 \text{ Hz}$, CH_2 , 2H), 2.14 (d,t $J_{\text{HCHg}} = 190 \text{ Hz}$, $J_{\text{HCCH}} = 7 \text{ Hz}$, CH_2Hg , 2H).

Octadecylmercury(II) *p*-Toluenesulfonate (2). Compound 1 (680 mg, 1.28 mmol) was dissolved in ethanol (99.5%, 100 mL) and silver *p*-toluene sulfonate (356 mg, 1.28 mmol) was added in one portion. The reaction mixture was stirred at room temperature overnight and filtered over celite. The solid was washed with ethanol (99.5%, 30 mL). The solvent was evaporated, and the product was recrystallized from petroleum ether. Yield 480 mg (60%). Mp $74 \text{ }^\circ\text{C}$. Elemental analysis: calcd.: 48.02% C, 7.09% H, 5.13% S, 32.08% Hg; found 47.90% C, 6.98% H, 5.10% S, 32.42% Hg. $^1\text{H NMR}$ (CDCl_3) δ 0.88 (t, $J = 7 \text{ Hz}$, CH_3 , 3H), 1.20–1.42 (m, s CH_2 , 30H), 1.70 (quintet, $J = 8 \text{ Hz}$, CH_2 , 2H), 2.23 (d,t $J_{\text{HCHg}} = 213 \text{ Hz}$, $J_{\text{HCCH}} = 8 \text{ Hz}$, CH_2Hg , 2H), 2.29 (s, $\text{CH}_3\text{--Ar}$, 3H), 7.13, 7.15, 7.48, 7.50, AB system, Ar).

Adsorbed Monolayer Formation. Glass substrates coated with 2000 \AA of gold were purchased from Platypus Technologies and were cleaned in one of two ways. In the first procedure, the gold substrates were cleaned by immersion in piranha solution (3:1 sulfuric acid/hydrogen peroxide) at $90 \text{ }^\circ\text{C}$ for 30 s, rinsed with copious amounts of $18.2 \text{ M}\Omega$ H_2O and absolute ethanol, and dried under a stream of nitrogen. In the second procedure, substrates were flame annealed prior to use with a hydrogen torch for ca. 30 s. Samples for XPS and STM measurements were prepared on gold on mica. Atomically flat Au(111) surfaces were obtained by flame annealing of the substrates.

Monolayers of 1-octadecanethiol were prepared by immersion of a gold substrate in a $1 \times 10^{-5} \text{ M}$ solution in absolute ethanol for $\sim 2 \text{ h}$. Octadecylmercury tosylate monolayers were formed by immersing the gold substrates in a $1 \times 10^{-3} \text{ M}$ or $1 \times 10^{-5} \text{ M}$ solution of an octadecylmercury(II) tosylate in dry THF for $\sim 2 \text{ h}$. After removal from solution, the gold substrates were rinsed three times with THF and dried under a stream of nitrogen prior to analysis.

Electrochemistry. Electrochemical measurements were performed using an Autolab PGSTAT302N potentiostat/galvanostat equipped with a frequency response module (Metrohm Autolab, The Netherlands). A four-electrode electrochemical cell for measurements of local properties of Au plates was constructed (SI, Figures S2 and S3). The design was aimed at measurements of voltammetry and electrochemical impedance spectroscopy in a small area of a plate coated with a gold layer. The cell can be moved to different locations on the Au plate for improved statistics. The working electrode was Au(111) deposited on a glass substrate, with a 0.64 cm^2 total area. It was mechanically attached to a microscope table equipped with two

manipulating screws enabling the choice of a spot on Au(111) to be electrochemically tested. The cell containing the solution was a glass tube mounted on a holder, which can be vertically moved with a fine thread screw. The lower part of the cell tube was fitted to a piece of Teflon with an O-ring. Two reference electrode wires were mounted through the Teflon body. The DC reference electrode was an Ag|AgCl wire. The high-frequency reference electrode was a Pt wire coupled to the DC reference electrode via a 0.1 μ F condenser. The distance between the two reference electrodes and the working electrode was approximately 1 mm. The auxiliary electrode was a Pt net mounted on a Pt wire and immersed in the cell tube through its upper end, which was closed by a septum. The area of the net was sufficiently larger than the working electrode area to meet the requirement for obtaining a cell impedance that corresponds to the impedance of the working electrode. Prior to measurements the cell tube assembly was moved down, gently pressed against the Au plate, and filled with the test solution. The entire setup showed no liquid leaks and a good reproducibility of the tested area. The adsorption and the compactness of adsorbed layers were followed by an established method using inhibition of electron transfer of the couple $[\text{Fe}(\text{CN})_6]^{4-/3-}$ in aqueous 0.1 M KCl or KNO_3 . Oxygen was removed from the solution by passing a stream of argon. Cyclic voltammetry was measured with a scan rate of the applied DC potential of 0.007 V/s. Inhibition or desorption was followed by changes of the kinetic parameters of the redox exchange of $[\text{Fe}(\text{CN})_6]^{4-/3-}$. Rate constants were evaluated by digital simulation using finite difference elements.⁴¹ Electrochemical impedance spectroscopy was measured in the range 100 kHz to 0.8 Hz using the amplitude of the AC signal 5 mV. The size of data collection was 120 points with a logarithmic distribution over the whole frequency range. Faradaic charge transfer resistance, reflecting quantitatively inhibition efficiency, was evaluated by a simulation program Nova 1.8 supplied by the manufacturer of the electrochemical instrument. Layers showing a high degree of inhibition were evaluated by voltammetry, whereas at low inhibition the impedance method proved to be more sensitive. The time dependence of the double layer capacity C of Au and glassy carbon (GCE) electrodes was measured using small electrode discs (0.5 mm diameter) sealed in a glass capillary. Phase-sensitive AC polarography used a sine wave of 64 Hz frequency and 10 mV amplitude. The change of C - E dependence during the adsorption process was measured in 0.1 M tetrabutylammonium hexafluorophosphate in acetonitrile. All solution components were dried.

Electrochemical stripping of Hg was performed by two different procedures with similar results. In the first one, samples were prepared by immersion of an Au plate that had been treated with $\text{C}_{18}\text{H}_{37}\text{HgOTs}$ into an electrochemical cell containing 0.1 M tetrabutylammonium hexafluorophosphate in acetonitrile and a specified potential was applied. In the other procedure, monolayers on a gold substrate were prepared by immersion of a clean Au plate into an electrochemical cell containing 0.1 M tetrabutylammonium hexafluorophosphate or aqueous 0.1 M KF and various amounts (0.05 to 0.2 mM) of $\text{C}_{18}\text{H}_{37}\text{HgOTs}$ in acetonitrile. Again, the potential was either applied or repeatedly scanned within selected limits.

Ellipsometry. All measurements were made using a variable-angle Stokes ellipsometer (Gaertner Scientific, U.S.A.) with a 633 nm HeNe laser with the incident angle adjusted to 70°. Optical constants of the gold substrates were taken for all freshly cleaned substrates. An index of refraction of 1.47 was assumed for the films. Ellipsometry measurements were taken at a minimum of five different areas on each sample.

Contact Angle Measurement. A static contact angle for 18.2 M Ω H_2O was found with a CAM101 instrument (KSV Instruments, Ltd., Finland) using a 1 to 2 μ L drop of water. Measurements were taken at a minimum of five different areas for each sample.

Infrared Spectroscopy. FTIR-ATR spectra (800 scans, 4 cm^{-1} resolution) were recorded using a Nicolet 6700 FT-IR spectrometer (Thermo Electron Corporation, U.S.A.) with a liquid- N_2 -cooled MCT detector in the range 650–4000 cm^{-1} . The data were collected with p-polarized light at 45° incidence using a Seagull variable-angle accessory (Harrick Scientific Products, Inc., U.S.A.) and a Ge hemisphere (12.5

mm diameter). Prior to each measurement, the Ge crystal was cleaned with ethanol and a reference spectrum of the crystal in contact with air was measured.

X-ray Photoelectron Spectroscopy. XPS was recorded with a Kratos Axis Ultra instrument using a monochromated Al K_{α} emission source (1486.6 eV) operated at 15 kV and 180 W. The photoelectrons were collected by the spectrometer in normal emission geometry. With an X-ray monochromator and a pass energy of 40 eV for the analyzer, an instrumental energy resolution of ~ 0.5 eV was achieved. The energy scale is referenced to the Au 4 $f_{7/2}$ line at a binding energy of 84.0 eV. For all samples, a survey spectrum and high resolution spectra of the Hg 4 d , Hg 4 f , S 2 p , C 1 s , O 1 s , and Au 4 f regions were acquired. The spectra were fitted using a linear background for all elements except Au and Hg, where Shirley background was used. Voigt functions employing a 50:50 Lorentz–Gaussian ratio, including a slight asymmetry factor (instrumental) were used as fit functions. The line shape parameters were determined by least-squares fitting to carbon or sulfur core level lines from known reference samples.

UV Photoelectron Spectroscopy. UPS was obtained using a helium UV lamp as a source. The gas pressure in the lamp was adjusted in such a way that He I ($h\nu = 21.2$ eV) and He II ($h\nu = 40.8$ eV) light was emitted in a ratio of approximately 4:1. The light was incident at an angle of 55° from the sample normal and the photoelectrons were collected by an energy dispersive hemispherical analyzer at a take-off angle of 90°. The analyzer was set to a pass energy of 5 eV, providing an instrumental resolution of about 0.14 eV. Binding energies were referenced to the Fermi level of a clean, argon ion-etched Au surface and defined as positive for occupied states below the Fermi level.

Monolayer Stability. The IR spectrum of each self-assembled monolayer was recorded. For stability measurements, the gold slide was immersed for 20–24 h at room temperature in dry CH_2Cl_2 , wet CH_2Cl_2 , n -hexane, ethanol, water, 0.1 M H_2SO_4 , 0.1 M NaOH, 1 mM KMnO_4 , 30% H_2O_2 , or 10 mM NaBH_4 , removed from solution, rinsed thoroughly with either an appropriate solvent (CH_2Cl_2 , n -hexane, or ethanol), or with copious amounts of 18.2 M Ω H_2O and absolute ethanol in the case of water solutions, and dried under a stream of nitrogen before an IR spectrum was recorded. The samples were also exposed to the ambient laboratory atmosphere for 7 days and then rinsed with absolute ethanol and dried before the IR spectrum was measured. Prior to the IR measurements, the gold slides were rinsed with absolute ethanol and dried under a stream of nitrogen.

■ ASSOCIATED CONTENT

📄 Supporting Information

Figures S1–S9 and a description of the electrochemical cell and equivalent circuit. This material is available free of charge via the Internet at <http://pubs.acs.org>.

■ AUTHOR INFORMATION

Corresponding Author

michl@eefus.colorado.edu

Notes

The authors declare no competing financial interest.

■ ACKNOWLEDGMENTS

The research leading to these results has received funding from the European Research Council under the European Community's Seventh Framework Programme (FP7/2007–2013 FUNMOL 213382 and ERC Grant Agreement 227756). Initial efforts were supported by the Grant Agency of the Czech Republic (203/07/1619 and 203/09/0705) and the Institute of Organic Chemistry and Biochemistry (RVO: 61388963). The authors thank Dr. P. Sajdl for performing additional XPS measurements, to Dr. Z. Bastl for a valuable discussion, and to Mr. P. Poncar for constructing a special electrochemical cell.

■ REFERENCES

- (1) Khobragade, D.; Stensrud, E. S.; Mucha, M.; Smith, J.; Pohl, R.; Stibor, I.; Michl, J. *Langmuir* **2010**, *26*, 8483.
- (2) Michl, J.; Stibor, I. CZ Patent No. 302441 B6, April 8, 2011.
- (3) Zheng, X.; Mulcahy, M. E.; Horinek, D.; Galeotti, F.; Magnera, T. F.; Michl, J. *J. Am. Chem. Soc.* **2004**, *126*, 4540.
- (4) Mulcahy, M. E.; Magnera, T. F.; Michl, J. *J. Phys. Chem. C* **2009**, *113*, 20698.
- (5) Mulcahy, M. E.; Bastl, Z.; Stensrud, K. F.; Magnera, T. F.; Michl, J. *J. Phys. Chem. C* **2010**, *114*, 14050.
- (6) Lee, T. R.; Whitesides, G. M. *Acc. Chem. Res.* **1992**, *25*, 266.
- (7) Kaletová, E.; Kohutová, A.; Si, Z.; Kaleta, J.; Scholz, F.; Hajduch, J.; Pospíšil, L.; von Wrochem, F.; Bastl, Z.; Michl, J. Book of Abstracts, 4th EuCheMS Congress, Aug. 26–30, 2012, Prague, Czech Republic, P-0888.
- (8) Cheng, Z. L.; Skouta, R.; Vázquez, H.; Widawsky, J. R.; Schneebeli, S.; Chen, W.; Hybertsen, M. S.; Breslow, R.; Venkataraman, L. *Nat. Nanotechnol.* **2011**, *6*, 353.
- (9) Chen, W.; Widawsky, J. R.; Vázquez, H.; Schneebeli, S. T.; Hybertsen, M. S.; Breslow, R.; Venkataraman, L. *J. Am. Chem. Soc.* **2011**, *133*, 17160.
- (10) Scholz, F.; Kaletová, E.; Stensrud, E. S.; Ford, W. E.; Mucha, M.; Stibor, I.; Michl, J.; von Wrochem, F., submitted for publication.
- (11) Love, J. C.; Estroff, L. A.; Kriebel, J. K.; Nuzzo, R. G.; Whitesides, G. M. *Chem. Rev.* **2005**, *105*, 1103.
- (12) Schreiber, F. *Prog. Surf. Sci.* **2000**, *65*, 151.
- (13) Ulman, A. *Chem. Rev.* **1996**, *96*, 1533.
- (14) Slowinski, K.; Chamberlain, R. V.; Bilewicz, R.; Majda, M. *J. Am. Chem. Soc.* **1996**, *118*, 4709.
- (15) Nuzzo, R. G.; Dubois, L. H.; Allara, D. L. *J. Am. Chem. Soc.* **1990**, *112*, 558.
- (16) Chidsey, C. E. D.; Loiacono, D. N. *Langmuir* **1990**, *6*, 682.
- (17) Bain, C. D.; Troughton, E. B.; Tao, Y. T.; Evall, J.; Whitesides, G. M.; Nuzzo, R. G. *J. Am. Chem. Soc.* **1989**, *111*, 321.
- (18) Protsailo, L. V.; Fawcett, W. R.; Russell, D.; Meyer, R. L. *Langmuir* **2002**, *18*, 9342.
- (19) von Wrochem, F.; Gao, D.; Scholz, F.; Nothofer, H. G.; Nelles, G.; Wessels, J. M. *Nature Nanotechnol.* **2010**, *5*, 618.
- (20) Colorado, R.; Villazana, R. J.; Lee, T. R. *Langmuir* **1998**, *14*, 6337.
- (21) Joseph, Y.; Guse, B.; Nelles, G. *Chem. Mater.* **2009**, *21*, 1670.
- (22) Willey, T. M.; Vance, A. L.; van Buuren, T.; Bostedt, C.; Terminello, L. J.; Fadley, C. S. *Surf. Sci.* **2005**, *576*, 188.
- (23) Huang, F. K.; Horton, R. C.; Myles, D. C., Jr.; Garrell, R. L. *Langmuir* **1998**, *14*, 4802.
- (24) Svenson, S.; Martensson, N.; Basilier, E.; Malquist, P. A.; Gelius, U.; Siegbahn, K. *J. Electron. Spectrosc. Relat. Phenom.* **1976**, *9*, 51.
- (25) Morris, T.; Szulczewski, G. *Langmuir* **2002**, *18*, 2260.
- (26) Chidsey, C. E. D.; Liu, G. Y.; Rowntree, P.; Scoles, G. J. *Chem. Phys.* **1989**, *91*, 4421.
- (27) Heyrovský, J.; Kůta, J. *Principles of Polarography*; Publishing House of the Czechoslovak Academy of Sciences: Prague, 1965, p 538.
- (28) Bard, A. J.; Faulkner, L. R. *Electrochemical Methods. Fundamentals and Applications*, 2nd ed.; John Wiley: New York, 2001, pp 286–293.
- (29) Koper, M. T. M. *Z. Phys. Chem.* **2003**, *217*, 547.
- (30) Li, J.; Abruna, H. D. *J. Phys. Chem. B* **1997**, *101*, 2907.
- (31) Chidsey, C. E. D.; Liu, G. Y.; Rowntree, P.; Scoles, G. J. *Chem. Phys.* **1989**, *91*, 4421.
- (32) Schmidt, R. W.; Reilley, C. N. *J. Am. Chem. Soc.* **1958**, *80*, 2087.
- (33) Weber, J.; Koutecký, J.; Koryta, J. *Z. Elektrochem.* **1959**, *63*, 583.
- (34) Kretschmer, R.; Schlangen, M.; Schwarz, H. *Angew. Chem., Int. Ed.* **2011**, *50*, 5387.
- (35) Risse, T.; Shaikhutdinov, S.; Nilius, N.; Sterrer, M.; Freund, H.-J. *Acc. Chem. Res.* **2008**, *41*, 949, and references therein.
- (36) Brown, M. A.; Ringleb, F.; Fujimori, Y.; Sterrer, M.; Freund, H.-J.; Preda, G.; Pacchioni, G. *J. Phys. Chem. C* **2011**, *115*, 10114.
- (37) Brown, M. A.; Fujimori, Y.; Ringleb, F.; Shao, X.; Stavale, F.; Nilius, N.; Sterrer, M.; Freund, H.-J. *J. Am. Chem. Soc.* **2011**, *133*, 10668.
- (38) Sridharan, R.; de Levie, R. *J. Phys. Chem.* **1982**, *86*, 4489.
- (39) de Levie, R. *Advances in Electrochemistry and Electrochemical Engineering*; John Wiley: New York, 1986; p 1.
- (40) Meals, R. N. *J. Org. Chem.* **1944**, *9*, 211.
- (41) BASi DigiSim Simulation Software for Cyclic Voltammetry; Bioanalytical Systems, Inc.: West Lafayette, IN, U.S.A.